Applications in Energy and Combustion Science 17 (2024) 100246

Contents lists available at ScienceDirect

Applications in Energy and Combustion Science

journal homepage: www.elsevier.com/locate/jaecs

Experimental investigation of multi-burner array with lean lifted spray flames in inline and inclined configurations

Mohamed Shamma *, Stefan Harth, Dimosthenis Trimis

Engler-Bunte-Institute, Division of Combustion Technology, Karlsruhe Institute of Technology, 76131 Karlsruhe, Germany

ARTICLE INFO

Keywords:
Flame characteristics
JET-A1
Lean burn
Lifted spray flames
Low swirl
NO_x emissions

ABSTRACT

Lean combustion in gas turbines garners attention for emissions reduction, yet it faces stability challenges demanding careful design considerations. In this study, a novel CHAIRLIFT combustor concept, which integrates low swirl lean lifted spray flames known for substantial nitrogen oxides emissions reduction, into a Short Helical Combustors (SHC) arrangement, is investigated. A comprehensive experimental test campaign explores key parameters, including staggered arrangement offset, equivalence ratios, and air inlet temperature, to evaluate its performance. The results reveal exceptional stability in low swirl, lifted flames compared to moderate swirl flames with larger inner recirculation zones. The unwanted flow deflection of highly swirled flames in the SHC arrangement is effectively avoided with the investigated low swirl, lifted flames. The study emphasizes the significant influence of fuel droplet evaporation time on flame stability near the flame root under low air inlet temperatures. Furthermore, at high air inlet temperatures, the complex flame stability mechanism in inclined configurations is controlled by various parameters, including outer recirculation zone size, air inlet temperature, and additional vortices generated by pressure differences near the wall. OH^* chemiluminescence results corroborate these stability mechanisms, showing that at lower temperatures, the flame stabilizes closer to the nozzle exit due to local rich pockets near the shear layer. Conversely, at the same tilt angle, higher air inlet temperatures lead to an increased flame lift-off height due to faster evaporation and enhanced mixing. Exhaust gas analyses confirm the potential of the investigated lean lifted spray flames in a multi-burner arrangement to achieve very low NO_x emissions over a wide range of operating conditions for all investigated burner inclinations. These findings may facilitate the future development and optimization of lean combustion technology for aircraft engines.

1. Introduction

Pollutant emissions, particularly those originating from aero-engines, have become a significant public concern due to their adverse environmental effects at both ground and high-altitude levels. To meet the long-term targets set forth in 'Flightpath 2050' by the Advisory Council for Aviation and Research in Europe (ACARE) [1], a substantial reduction in aircraft pollutant emissions is imperative. Lean-premixed combustion technology, initially introduced by Lefebvre [2] and Correa [3], holds the potential to minimize nitric oxide emissions by controlling the composition of the fuel/air mixture and, consequently, the flame temperature. The primary challenge associated with implementing a lean-burn strategy lies in its potential impact on engine operability. Lean combustion typically operates near the lean-blow-off limits, rendering the combustion process inherently susceptible to thermoacoustic instabilities or complete flame extinction, which can result in severe structural damage or reduced system lifetime. In contemporary combustion devices, lean-premixed flames stabilized in swirling flows are widely employed due to their effectiveness in minimizing nitric oxide emissions. However, achieving a sufficient degree of premixing before combustion, especially under non-premixed conditions with liquid fuels, remains a daunting task.

Swirling flow burners play a pivotal role in both premixed and non-premixed combustion systems, exerting a substantial influence on flame stability, combustion intensity, and overall combustor performance. The characterization of the degree of swirl in a given flow field is captured by the swirl number, introduced as the dimensionless ratio of axial flux of angular momentum to the axial flux of axial momentum by Gupta et al. [4]. The examination of swirl flow behavior and the impact of swirl number on flow structure has been undertaken by various researchers, commencing with early investigations by Chigier et al. [5]. These studies elucidated the effects of swirl number on flow structure, revealing that the sudden expansion in confinement gives rise to a corner vortex known as the outer recirculation zone

* Corresponding author.
E-mail address: mohamed.shamma@partner.kit.edu (M. Shamma).

https://doi.org/10.1016/j.jaecs.2024.100246
Received 15 September 2023; Received in revised form 14 December 2023; Accepted 3 January 2024
Available online 9 January 2024

(ORZ). Furthermore, an increase in swirl number to a certain threshold induces the formation of a vortex, termed the inner recirculation zone (IRZ), also recognized as a vortex-breakdown phenomenon. Numerous studies, encompassing both experimental and numerical approaches, have explored the influence of swirl intensity on flow behavior and combustion dynamics. Tsao et al. [6] simulated a gas turbine combustor using a can model for varying swirl numbers forming a vortex core whose strength depends on the inlet swirl levels. Stone et al. [7] numerically investigated the impact of three swirl numbers on the stability of a lean-premixed gas turbine combustor, observing vortex-breakdown for high swirl numbers, indicated by negative centerline axial velocity in the expansion plane. Anacleto et al. [8] conducted experimental investigations on a lean premixed burner with adjustable vanes, revealing the occurrence of vortex-breakdown at a specific swirl number of 0.5. Ying and Vigor [9] utilized Large-Eddy Simulation (LES) techniques to examine the influence of swirling flow on combustion dynamics. They reported that when the swirl number surpasses a critical value of 0.44, vortex-breakdown occurs, leading to the formation of an IRZ. Martin et al. [10] recently explored the impact of swirl number on the structure of swirl-stabilized spray flames, varying swirl number through changes in swirler configuration. They observed that combustion stability and flame lifting behavior were contingent on the swirl intensity of the flow.

In modern gas turbine combustors, the usage of high-swirl fuel nozzles is well-established and reviewed by Syred et al. [11]. Johnson et al. [12] conducted tests on high swirl (HSI) and low swirl (LSI) flows in a simulated gas turbine environment, up to full load conditions of typical 5–7 MW engines. They observed that the flames produced by the low swirl configuration remained stationary despite changes in inlet temperature and pressure. The LSI emits NOx levels about 60% lower than those from the HSI and has no effect on CO emissions. These results strongly suggest that LSI is a promising, simple, and cost-effective solution for gas turbines to achieve ultra-low emissions targets of <5 ppm NOx.

Low swirl burners, as developed by Cheng et al. [13], in contrast to high swirl burners, tend to produce weak vortex breakdown and recirculation zones. Consequently, the flame is typically stabilized at a higher lift-off height from the burner nozzle, which can be helpful for preventing the flame from flashing back and overheating the burner as well as to improve the degree of premixing. Understanding the dynamics of lifted flames and the factors influencing blowout is crucial for flame stabilization. Various theories aim to elucidate this phenomenon in turbulent jets. A subset of these theories focuses on the interaction between turbulent eddies and premixed flame fronts, anchoring the lifted flame through complex turbulent dynamics [14]. Alternatively, other perspectives highlight the influence of large-scale turbulence structures on lifted flame characteristics [15]. Additionally, some theories consider the extinction of laminar diffusion flamelets as a contributing factor to lifted flame behavior [16]. These complementary theories collectively contribute to a comprehensive understanding of the mechanisms governing flame stabilization in turbulent jets.

Even though many studies have been performed on lifted flames for gaseous fuels, not all phenomena related to these flames are yet fully understood. Singh et al. [17]. assessed flame stability and spray characteristics over a wide range of Weber numbers and dynamic pressure ratios using the Sydney needle burner (SYNSBURN) with air-blast atomization. Various fuels and needle sizes were tested for different equivalence ratios, Weber numbers, and dynamic pressure ratios. The study reveals that peak flame stability is achieved at an optimal equivalence ratio, which is dependent on the Weber number and, consequently, the quality of the spray. Results on liquid fuels are available, but mostly related to more fundamental experiments and self-ignition [18].

Technical relevant systems for lifted jet flames with liquid fuels are scarce. Lifted spray flames for application in aero-engines as well as stationary gas turbines that operate under extremely lean conditions were further developed at Karlsruhe Institute of Technology under the CHAIRLIFT project as presented in detail by Shamma et al. [19]. In the presented staggered combustor, the short helical combustor (hereafter named SHC) approach as described by Ariatabar [20] is combined with the adoption of low swirl lean lifted spray flames presented by Kasabov [21] after adapting the nozzle/combustor expansion ratio applicable for medium size engines. By joining these two innovative combustion strategies, it is targeted to develop a new combustor concept suitable to accomplish the long-term targets for NOx emission reduction in aero-engines. The present experimental study focuses on the detailed characterization of the combustion process of the multi-burner array at different staggered angles (0, 20, and 45). Flow field, fuel spray, flame structure and location, temperature field, flame stabilization mechanism, and emission performance along a wide range of operating conditions (air inlet temperature 290 to 673 K and air flow rate, defined by air pressure drop across the nozzle between 1% and 4% of the air supply pressure) of spray jet flame by combining advanced optical diagnostics and probes measurement. The velocity field is obtained by the Particle image velocimetry (PIV) technique. Utilizing the same measurement arrangement, spray droplet dispersion is measured by the Mie-Scattering phenomenon. OH* chemiluminescence technique is used to characterize the flame structure of spray flame. Exhaust gas sampling by probes was employed to evaluate the emission performance at different operating conditions and a point-based thermocouple probe was utilized to obtain the temperature distribution to gain insights into the complex flow interactions between the burners.

2. Experimental set-up

In the following sections, a detailed explanation of the test rig facility, measurement techniques, and the combustor configurations used in this study are presented.

2.1. Optical setup

In this section, an overview of the test rig facility and equipment used to investigate the combustion characteristics of multi burner array mounted in different arrangements as shown in Fig. 1 is presented. The experimental investigations were carried out in a multi-burner array test rig consisting of five modular burners operated at atmospheric pressure. The burner array has the flexibility of changing the inclination angle (or the vertical distance between the burner domes) which allows operating the test rig at inline (0°) and staggered/inclined (20°, and 45°) as depicted in Fig. 2 in order to study the effect of flame interactions on the combustion characteristics. With no burners inclination, the inline configuration reproduces a sector of a simplified conventional annular combustor, while the staggered configuration represents the novel helical combustor concept [20]. Each particular burner of the array has a square cross-section base plate of 100 × 100 mm and a combustor height of 300 mm relative to each nozzle exit.

The air plenum for each nozzle has an inner diameter of 68 and 435 mm in length and includes a flow straightener plate used to enhance symmetry to the inlet velocity profiles. Combustion takes place in the combined chamber of the burners array, where the adjacent flames are free to interact. 2 mm thick quartz glass windows delimit the combustion chamber, allowing wide optical access (174 × 302 mm^2) to the interaction regions of the neighboring flames. The exhaust of the combustion chamber is open to ambient air with outlet contraction to avoid any interruption with the ambient air. Liquid jet A-1 fuel was utilized in the experiments to mimic real aircraft engine conditions. Prefilming air-blast nozzles shown in Fig. 3 are widely used in practical modern gas turbine engines due to fine fuel atomization and only small changes in performance over a wide range of operating conditions.

The total airflow rate is measured by a thermal flow meter with an accuracy of 0.5% of full scale output. The compressed air was preheated by an electric air preheater which raised the air inlet temperature up to

Fig. 1. Photograph of the experimental setup including an optical measurement techniques employed in the investigations.

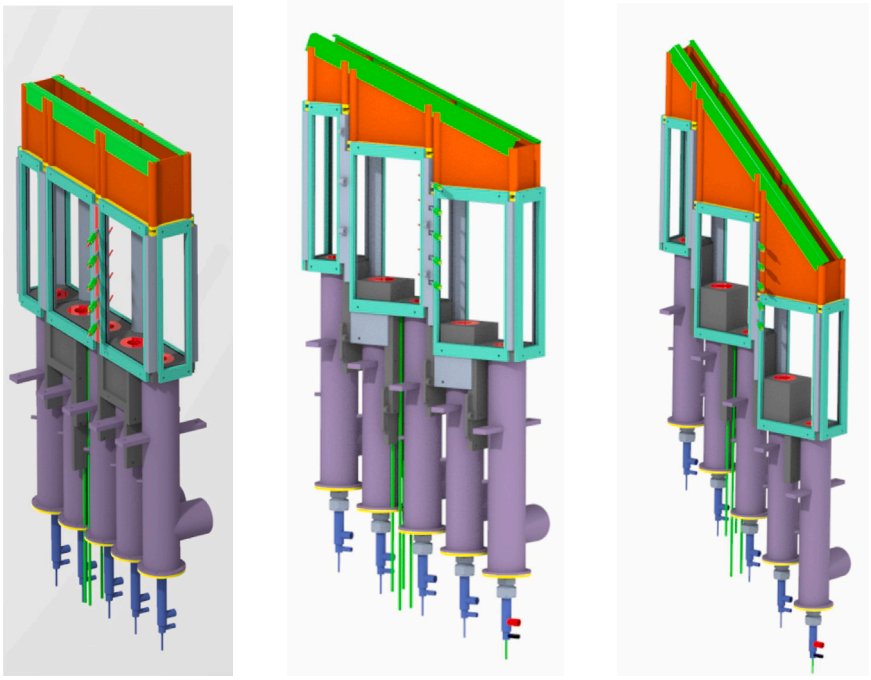

(a) Inline (θ =0°). (b) Inclined (θ =20°). (c) Inclined (θ =45°).

Fig. 2. Schematic of modular burner array at different arrangement.

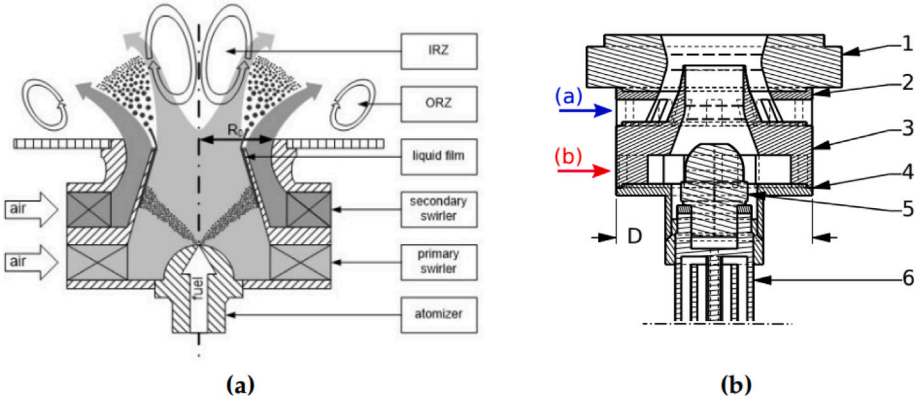

Fig. 3. (a) Air-blast atomization process [22]. (b) Scheme of the investigated nozzle type, where: (1) Diffuser, (2) Secondary Swirler, (3) Primary Swirler, (4) Inlet, (5) Atomizer, (6) Fuel Feeding Lance, (A) Secondary Air And (B) Primary Air.

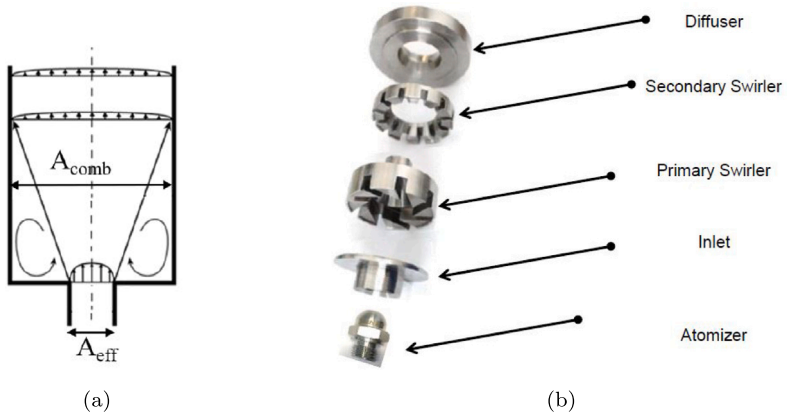

Fig. 4. (a) Geometrical parameters for expansion ratio definition. (b) Picture of air blast nozzle parts.

Table 1
Summary of operating conditions for all the experiments.

Parameter	Value	Unit
Configuration angle	0°, 20°, 45°	
Air inlet temperature	290, 373, 473, 573, 673	K
Individual burner air flow rate range	10.3–30.7	g/sec
Operating pressure	1.0	bar
Equivalence ratio	0.39–0.82	[–]
Individual burner power	11.9–71.6	[kW]

400 °C. After passing inside the preheater, the airflow rate going to the system was regulated with gate control valves. The air then fed to an air distributor to provide a uniform and equal airflow to all the burners. Jet-A1 fuel mass flow was measured by Coriolis mass flow meters to control the fuel flow rate for each burner separately, with an accuracy of 0.1% of the measured value. To capture a wide range of aircraft engine-like operating conditions, several flow parameters have been varied in investigations, such as the air inlet temperature, air pressure drop across the nozzle (or related air flow rate), and equivalence ratio. The operating conditions of the test campaign for the multi-burner array at different arrangements are illustrated in Table 1.

2.2. Configuration of air-blast nozzle

Swirling flows are commonly used to stabilize gas turbine combustion at high heat release rates. Low swirl flow is particularly advantageous in combination with the SHC geometry to avoid the unwanted flow deflection [19]. Optimizing geometrical parameters is crucial to achieve high-performance requirements, including reducing pollutant emissions and improving combustion efficiency and flame stability. Low swirl flow is generated by inserting a set of guide vanes (known as a swirler or swirl generators) within the burner to provide tangential velocity component to the flow. The nozzle design is based on the one used by Kasabov et al. [21], composed by double swirlers (primary and secondary) with an outer diameter D = 50 mm. Fig. 4(b) present the nozzle components. Primary swirler consists of eight tangentially inclined vanes, with an eccentricity of 10,3 mm. The secondary swirler has twelve straight vanes at zero trailing angle, thus without adding any tangential component to the flow. The prefilmer lip separates the primary and secondary air flows, and has a final thickness of 0.35 mm, which is a crucial parameter for the atomization performance. Among the design parameters considered, nozzle effective area (A_{eff}), expansion ratio between nozzle and combustor cross section Δ, and swirl strength has a notable impact on the size and the shape of the inner and the outer re-circulation zones and accordingly on the flow field and combustion process. The effective area of a nozzle, which is smaller compared to the geometrical area due to losses, allows to calculate the mass flow based on thermodynamic conditions. The value of A_{eff} has been selected according to the results of Kasabov [21] as 319 mm^2.

The expansion area ratio Δ, defined as the ratio between the combustor cross section area A_{comb} to the nozzle effective area A_{eff} are shown in Fig. 4(a). Δ is a critical parameter that contributes to the formation of a recirculation zone resulting from vortex breakdown, which is caused by the sudden expansion of a swirling flow. Δ = 31.3 was chosen as it is considered as a realistic expansion ratio for combustors in aero-engines.

Swirl number (SN) is used to characterize the rotating axial flow in the burner to characterize the strength of the swirling in relation to the axial flow. Swirl number is defined as the ratio of the axial flux of angular momentum $\dot{D}$ to the axial flux of the axial momentum $\dot{I}$ multiplied by characteristic length (1). The nozzle radius R_0 at nozzle exit was used as characteristic length in the Swirl number definition. The primary swirler utilized in this nozzle has a SN of 0.76 however the secondary swirler with zero trailing angle and zero swirl number.

$$S = \frac{\dot{D}}{\dot{I} \cdot R_0} \tag{1}$$

2.3. Measurement techniques

To gain insights into the combustion characteristics of the inclined burner combustor concept, a comprehensive analysis of key parameters such as temperature, velocity field, fuel spray penetration, and emission formation is essential. This section outlines the instrumentation and methodologies employed for these investigations. Two-dimensional PIV measurements were performed using a diode pumped, dual cavity, high-speed Nd:YLF laser (Litron LD25-527 LM2827) together with a high-speed camera (Phantom V1212, resolution 1280 × 800 pixels) set to 5 kHz recording frequency (double frames at maximum resolution). 1000 double frame images were recorded per measurement for total measurement time 200 ms and the time separation between the laser pulses was set to 20 μs. The camera was calibrated and focused using a rectangular target with 5 mm dot spacing centered at the fuel nozzle. Aluminum oxide particles (Al_2O_3) with a particle size of 1 μm were employed as seeding material and introduced into the air flows for each burner using fluidized bed seeders. The Aluminum oxide seeding particles were dried overnight prior to each measurement. A 532 nm bandpass optical filter is used to filter the undesirable light. The field of view (FOV) for the PIV measurements are focused on the two center burners. Depending on the height of the laser light sheet (100 mm) and the resolution of the camera, the FOV is divided into two axial parts (PIV#1 and PIV#2) in Fig. 5. Velocity field calculations were performed using a commercial PIV software (DaVis 10.2, LaVision). Pictures were preprocessed by subtracting the background and masking off all reflection zones near to the burners domes. Cross correlation started at 48px window size and 50% overlap decreasing to 32px

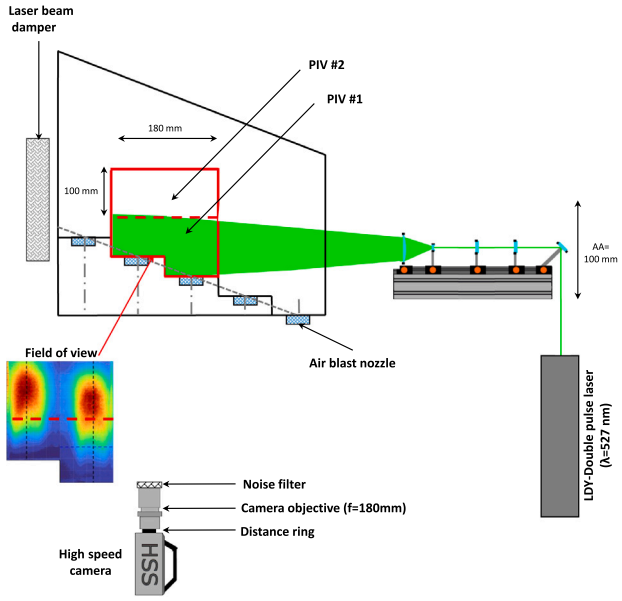

Fig. 5. Schematic depicting the 2D PIV arrangement and the laser sheet.

window size and 50% overlap. Utilizing the same measurement setup, Mie scattering laser diagnostic technique was applied to get a deep insight into the spray characteristics affecting the flame characteristics including penetration depth of the fuel spray into the flame and the hollow cone angle of the spray. In order to analyze the composition of the exhaust gas, a sample gas stream was extracted by a water-cooled exhaust gas sampling probe with 12 mm outer diameter. The water/glycol mixture for cooling of the probe was kept at 85 °C to avoid condensation of water. The temperature measurements inside the combustor were conducted using a thermocouple consisting of a metal sphere of 0.4 mm diameter at tip. The first 100 mm of the thermocouple are non-cooled and the two wires from the metal sphere are housed by a ceramic tube with 2 channels and an outer diameter of 3.5 mm. In order to minimize the impact of the probe on the flow field, only the thermocouple holder, which starts 100 mm downstream of the probe tip is water-cooled and has an outer diameter of 12 mm. As invasive measurement technique, thermocouple measurements are prone to errors due to their impact on i.e. the flow field and the flame. Nevertheless, the applied thermocouple type/size is considered as appropriate tool for a qualitative analysis of different configurations.

3. Results and discussion

The present study conducts a comprehensive investigation of the effect of burner arrangements, specifically burner inclination angles, combustion characteristics. The results are presented with a detailed analysis of the flame stabilization mechanism at various operating conditions and inclination angle in Section 3.1. This includes an examination of the impact of air inlet temperature on the structure and position of lean flames in Section 3.2. Additionally, the final section, Section 3.3, includes analysis of the burner's emission performance under different conditions, enhancing the understanding of the effect of burner arrangement on kerosene/air flame structure and stabilization in a multi-burner, low swirl burner configuration under ultra-lean conditions.

3.1. Lean blowout limits of the CHAIRLIFT concept

The stability range of a combustor is essential for safe operation of an engine, as well as has a direct impact on pollutant emissions. A wide

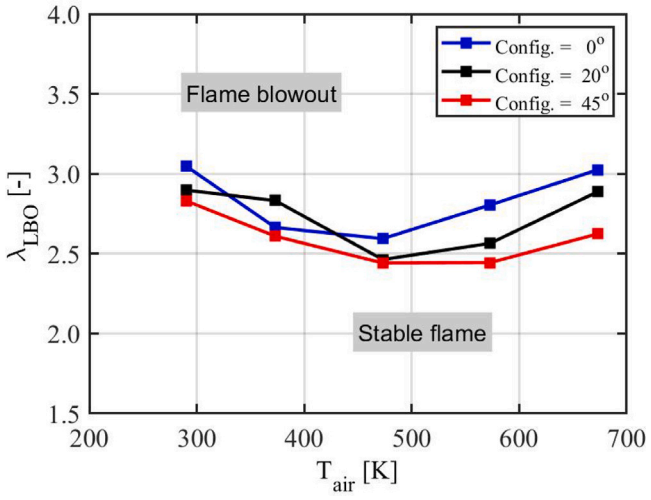

Fig. 6. Effect of air inlet temperature on lean blowout limits for different configurations at the same air pressure drop 3%.

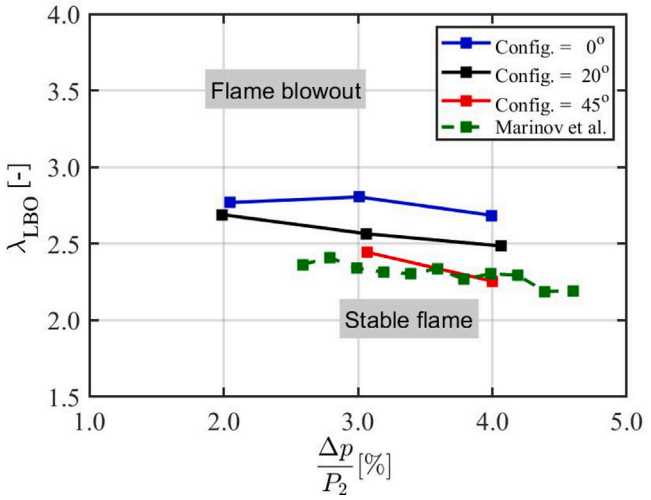

Fig. 7. Effect of air pressure drop on lean blowout limits at the same air inlet temperature 573 K compared to moderate swirl investigated by Marinov et al. [24].

stability range enables the combustor to operate at low combustion temperatures, resulting in very low NOx emissions for the majority of cycle conditions. Blowout, a phenomenon commonly described as a loss of stability, occurs when the flame inside a combustor is blown off as a result of e.g. local extinction due to high instantaneous strain rate. This can have serious consequences on the engine performance and safety. Thus, understanding and controlling the stability range of the combustor is crucial for the safe and efficient operation of the engine, as well as for reducing pollutant emissions [23].

In this research, the lean blowout (LBO) limit is defined as highest possible excess air ratio before extinctions or blow out. The LBO measurements helps in obtaining the minimum fuel flow rate for a particular engine conditions below which the flame cannot sustain itself. This can be helpful in finding the operating range of low swirl flow for different configurations. The LBO measurements are performed starting from stable conditions, that is maintained for a sufficient time, the air flow rate is kept constant while the fuel flow rate is lowered slowly in steps until the central flame is completely extinguished. To prevent premature blowout resulting from heat loss, the on-side burners were operated 8% more fuel rich, which resulted in the middle burner extinguishing first.

3.1.1. Impact of the air inlet temperature

The lean blowout limits of the lifted low swirling flames at different operating conditions are shown in Figs. 6, and 7. Fig. 6 illustrates the effect of air inlet temperature (T_{air}) on the flame stability limits of low-swirl, turbulent non-premixed Jet A1-air flames at different tilt angles. In this Fig., λ_{LBO} is the air number ($\lambda_{LBO} = 1/\phi_{LBO}$) at the blow-out conditions where the stable conditions are achieved for the values below each line. It can be noted that at low air inlet temperature (≈ 290 K) the flames have a very good stability performance for all burners alignments and pressure drops. The measurements of the fuel spray (as depicted in Fig. 10) show that under these low temperature conditions fewer droplets pre-evaporate upstream near the burner dome and large droplet migrate outward due to centrifugal force causing localized enrichment in the shear layer zone near to the outer recirculation zone (ORZ) where the swirl lifted flame stabilizes. Fig. 10 presents the averaged data from various measurements, encompassing the flow field, spray, and flame structure. The averaged OH* images undergo processing via an inverse Abel transform algorithm to resolve integrated line-of-sight data distribution to a specific azimuthal plane. For the applied Abel transformation, rotational symmetry of the flame was assumed as an approximation. Potential errors due to asymmetries of the flame have to considered when analyzing the presented results. By increasing the air inlet temperature to 473 K and maintaining a constant air pressure drop of 3% across the nozzle, the fuel evaporation time decreases. This results in better mixing and a higher degree of premixing and pre-evaporization. This can be observed in Fig. 10, which shows that the fuel spray and reaction zone are well separated. In consequence, most of the droplets evaporate near to the nozzle axis and far away from the ORZ which reduces the flame stability but it is very promising behavior regarding emission performance.

Further increasing the inlet air temperature to the highest level (≈ 673 K) at the same air pressure drop, increases the flame stability due to the increase in the flame speed compared to the increase of the flow velocity which could be explained by the premixing theory [25]. According to the premixing theory, lifted flames stabilize in a turbulent regime where the stoichiometry is dictated by the balance between the gas flow velocity U_{air} and the turbulent burning velocity S_T at the flame stabilization point. The velocity of the jet stream leaving the nozzle obeys the gas-dynamic equation and changes with the air inlet temperature as $U_{air} \propto \sqrt{T_{air}}$. Due to the square-root dependency, the increase in the jet exit velocity with the temperature is more pronounced at lower temperatures and flattens out at higher temperatures. However, the laminar burning velocity has a quadratic dependence ($S_L \propto {T_{air}}^2$). Thus, the increase in burning velocity is greater than the increase in inflow speed shifting the location of the reaction zone upstream and enhances the flame stability. An additional factor that plays a role in flame stabilization of such low swirl flame is the size of the outer recirculation zone as described by Kasabov et al. [21]. From the flow field measurements at different air inlet temperatures, the size of ORZ is estimated in Fig. 9 by calculating the area bounded by the zero axial velocity line. As we can see, size of the outer recirculation zone, measured in 2D plane, increases linearly with air inlet temperature, pushing the low velocity shear layer towards the nozzle axis where the flame stabilizes.

3.1.2. Impact of the inclination angle (different offsets)

The particular focus of this research is to study the influence of the tilt angle on the flame stabilization limits and stabilization mechanism to evaluate this innovative helical-arranged burner array and compare it to the inline arrangement as a representative of the conventional annular combustor at different operating conditions. Fig. 7 shows a good stability range of lifted flames despite the high degree of premixing (similar or even better lean-blow-out compared to typical moderate swirl stabilized flames with big inner recirculation zone for lean injection systems investigated by Marinov et al. [24]). A comparison of the lean stability limits for different orientations showing the integration of

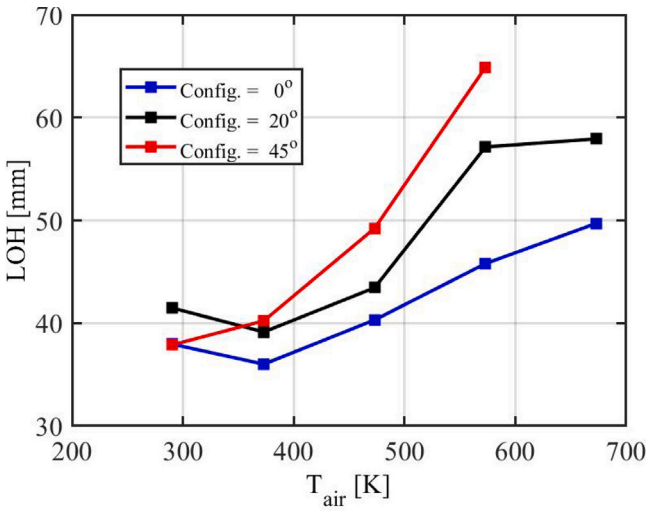

Fig. 8. Effect of air inlet temperature T_{Air} on flame position/liftoff height for different burner array arrangement.

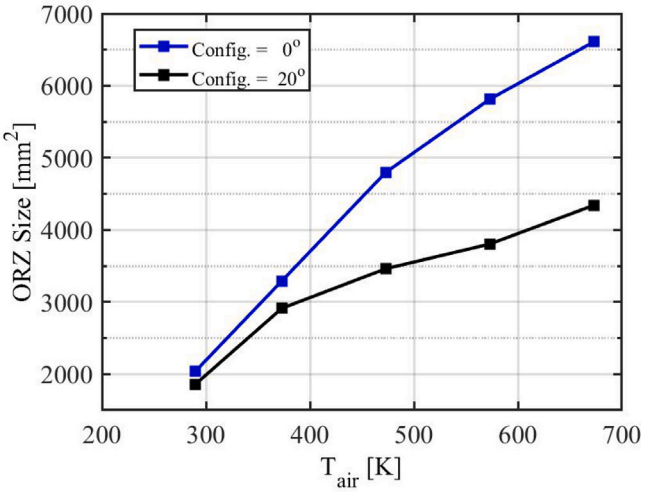

Fig. 9. Effect of air inlet temperature on the size of outer regulation zone for different configuration.

lifted flames into the helical arrangement for two different tilt angles (20°, and 45°) as solid black and red lines respectively in Fig. 7, and the inline arrangement 0° is shown as a solid blue line. This figure shows that in all cases the flame stability margins have a similar trend with increasing the air inlet temperature but are different in magnitude. The interesting observation here is that the flame stability at low air inlet temperatures (near the idle engine conditions) is controlled via way of means of the slower evaporation of the fuel droplets creating locally rich pockets near the flame root as explained in the previous Section 3.1.1 and with a little impact of the alignment of the burner. At high air inlet temperatures, the blow-off limit of the inline case is surprisingly higher than with staggered arrangements. The present results reveal that the blow-off limit is inversely proportional to the tilt angle at higher air inlet temperatures. PIV and temperature measurements were performed in order to characterize the reacting flow field and hence help the understanding of the aforementioned flame features/observations.

It is clear that in Figs. 10 and 12, under all conditions of the inline arrangement, the flow field structure is dominated by the ORZ at the sides of each individual burner. The size and location of these ORZs are dependant on the ratio of air inlet temperature to adiabatic flame

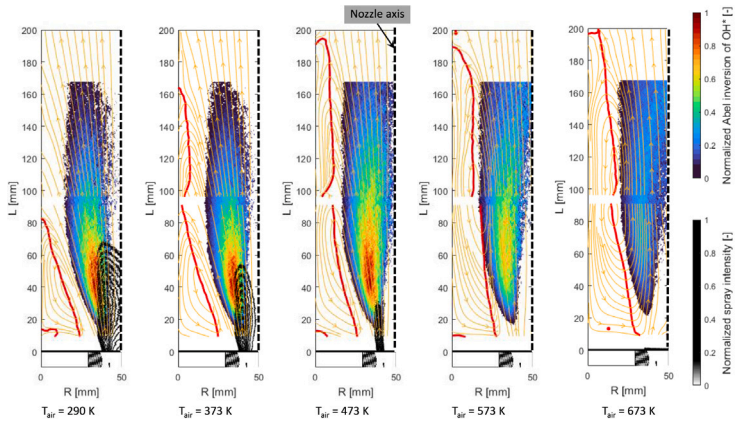

(a) Inline

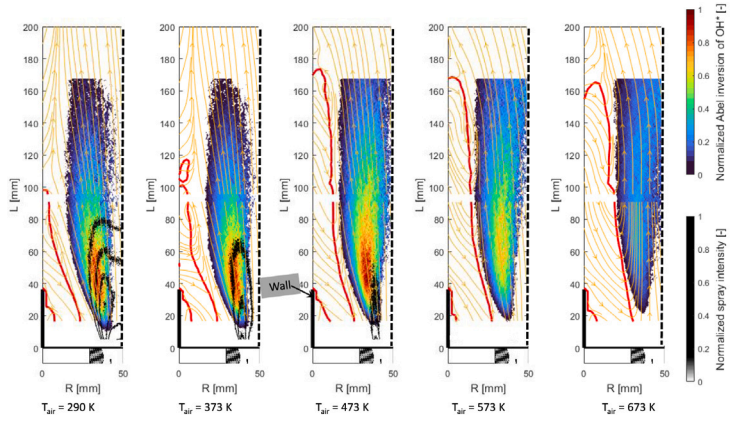

(b) Inclined (20°)

Fig. 10. Contour plot of ensemble OH signal at constant $\phi = 0.5$ and $\frac{\Delta p}{P_2}$ = 3%, color contours show flame structure, black contours show fuel spray, red line shows recirculation zone, yellow stream lines show axial velocity and black dash line shows nozzle center. (For interpretation of the references to color in this figure legend, the reader is referred to the web version of this article.)

temperature (T_{air}/T_{ad}) which determines the flow expansion inside the combustor. The recirculation zones cause low-velocity regions where the flame can anchor. Additionally, it acts as a radical pool and thermal reservoir which helps the heat transfer from the flame to the fresh mixture upstream of the lifted flame base, and the resulting flame speed is increased, as well as increasing the level of turbulence which helps the flame to stabilize. The size and the temperature of the outer recirculation zone are very important parameters in the stabilization of this lifted low swirl flame consistent with the previous investigations of Kasabov et al. [21]. The estimated size of ORZ shown in Fig. 9 shows that the stabilization of the inline case is enhanced at elevated T_{air} due to the significantly larger ORZ. The measured temperature profiles in a reactive flow for the different alignments shown in Fig. 11 suggest an unexpected decrease in flow temperature of the staggered case near the wall which decreases the temperature at one side of ORZ due to the recirculated airflow from the upper burner to the lower one. The effect of the stepped wall in the staggered case on the recirculated flow between the adjacent burners is illustrated in more detail in Fig. 13.

According to these PIV measurements, there is a portion of the cold flow (shown by the green arrows in the schematic in Fig. 13(b)), moving from point 1 at the open side of the higher burner to point 2 near the wall of the lower burner. This flow is driven by the pressure difference between free jet with low stream velocity and high pressure at the open side of the higher burner and confined jet with high stream velocity and low pressure near the wall of the lower burner. This flow stream isolates the ORZ on the wall side and prevents it from contributing in the flame stabilization process. On the other side, there are another two small RZs (red arrows) that arise due to the flow expansion and differences in flow direction, which are compensate for the ORZ near the wall and help the flame to stabilize. In short, while the helical arrangement does add complexity to the flow field, the basic flame stabilization process is still controlled by the ORZs.

3.1.3. Impact of the pressure drop across the nozzle

The effect of the pressure drop across the nozzle on the flame stability at constant air inlet temperature (573 K) and for different burner arrangements is shown in Fig. 7. For all cases studied, increasing the pressure drop negatively impacts the flame stabilization either for the inline or the staggered configurations. The gas-dynamic equation is once again invoked to correlate the air pressure drop with the air inlet velocity through the following dependency ($\frac{\Delta P}{P_2} \propto {U_{air}}^2$). By increasing the pressure drop, the air velocity at the relevant locations for atomization and i.e. at the edge of the prefilmer rim increases and the fuel atomization is improved. As a result, fast air/fuel mixing is achieved near the burner dome, and only a minor amount of non-evaporated droplets is present near to the nozzle axis and far away from the outer recirculation zone, which plays the dominant role in the flame stabilization of low swirl flames.

3.2. Flame structure

The inherent structure and location of the turbulent flames are of great importance and need to be investigated to fully understand the combustion characteristics of the helical arrangement. Qualitative

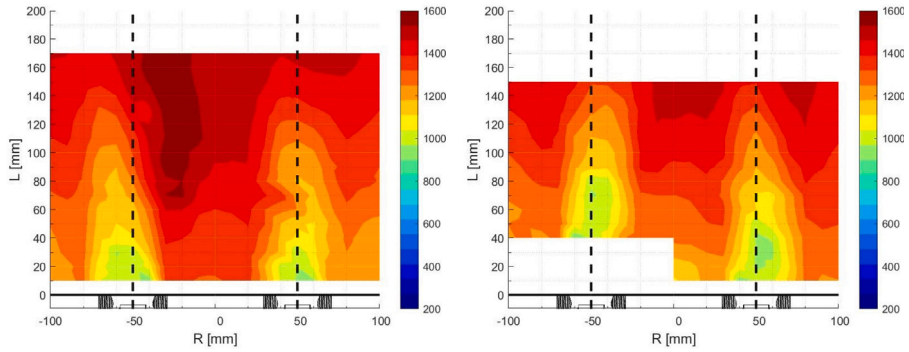

(a) Inline (b) Staggered/Inclined (20°)

Fig. 11. Contour plot of temperature distribution across the vertical nozzle mid plane for different configurations.

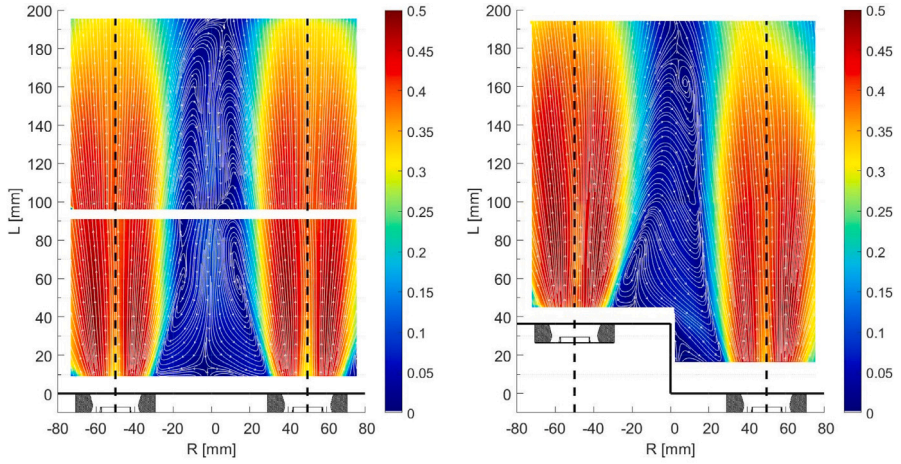

(a) Inline (b) Staggered/Inclined (20°)

Fig. 12. Contour of mean velocity magnitude overlaid with streamlines in the vertical axial midplane of the burners for different configurations.

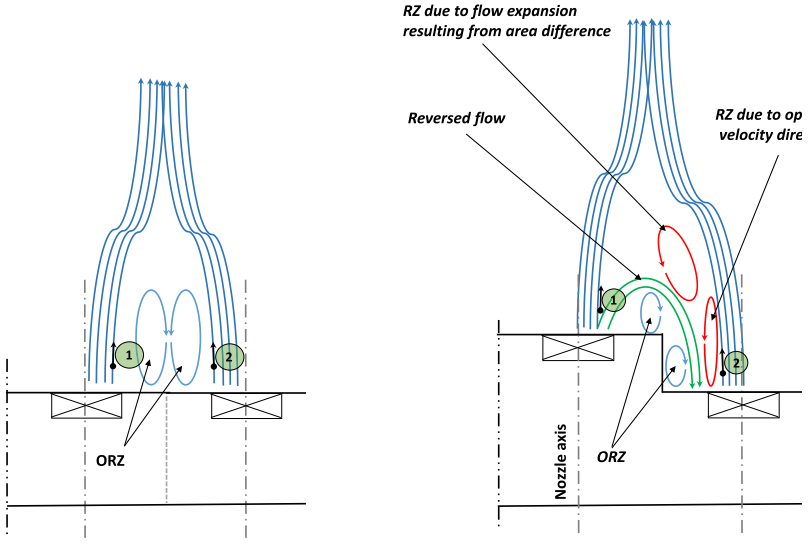

(a) Inline (b) Inclined

Fig. 13. Effect of air inlet temperature on flame lift off height.

measurements of OH* chemiluminescence were performed at the axis of the central burner to visualize the main reaction zone. A synthesis of the flame structure, containing the half-plane center burner flow field, the spatial distribution of the flame reaction zone (Abel-transformed OH* chemiluminescence from 1000 averaged line-of-sight images) and time average fuel spray distribution of the inline and staggered/inclined (20°) configurations is shown in Fig. 10. At lower air inlet temperatures, OH* chemiluminescence images reveal conspicuous, high-luminosity heat release zones situated outward on each side of the nozzle center. These zones result from the outward movement of droplets near the shear layer, influenced by the fuel's physical properties, particularly in lower temperature (T_{air}) air conditions, which impede the evaporation of the droplets.

Fig. 10 depicts the flame structures of each configuration under different T_{air}. By increasing T_{air} the actual heat release region distributes mildly around the axis of the nozzle where fine fuel droplets with evaporated fuel accumulate and good mixing with the air is reached.

The lifted type of flame is integrated into the staggered arrangement where the flame is not anchored to the injector. The main parameter for enhancing the mixing process is the lift-off height. The lift-off height (LOH) extends the time for evaporation and mixing. The lift-off height is defined as the distance from the jet outlet to the flame base. Lift-off height is of crucial importance, not only because of the direct impact on flame stabilization but also because can be used to explain the emission performance. In this study, the lift-off height was determined based on high speed OH* chemiluminescence measurements and defined as the distance between the nozzle exit and the horizontal line upstream of which 10% of the total chemiluminescence intensity is present as explained by our previous research [19]. Fig. 8 shows the variations of lift-off height (LOH) with air inlet temperature studied for different configurations. It is evident that at lower temperatures and for all configurations, the flame stabilizes at a smaller distance above the nozzle exit resulting from the local rich pockets near the shear layer. For the same tilt angle, the flame lift-off height increases with increasing the air inlet temperature due to faster evaporation and the related higher degree of mixing. The higher degree of mixing is compatible with the mentioned stability mechanism. Increasing the air inlet temperature to a certain point (based on each tilt angle) results in a lower ratio of flow velocity to burning velocity, the flame position will adapt and move downstream.

3.3. Emissions performance

In the previous section, the combustion characteristics, including the flame structure and stabilization mechanism, of helical and annular modular combustor arrays were investigated at different operating conditions. To fully asses the innovative staggered combustor arrangement, the environmental impacts i.e. Carbon monoxide (CO) and Nitrogen oxides (NOx) emissions for the steady state operating conditions were also recorded and analyzed under different operating conditions. In all the following discussion, pollutant concentrations in the exhaust gas are expressed in the form of emission indices. The emission index indicates the amount of the respective pollutant released during the combustion of a given amount of fuel, and defined by

$$EI_i \equiv \frac{m_{i,\text{emitted}}}{m_{f,\text{burned}}} \quad \text{g/kg} \tag{2}$$

One advantage of reporting emissions as an emission index is that it can be directly linked to the performance of the gas turbine, which is associated with fuel consumption. In the case of hydrocarbon combustion, the emission index can be calculated from the mole fractions of the pollutant and all carbon-containing species in the exhaust gas as defined in SAE ARP 1533 guidelines [26] . Neglecting unburned hydrocarbons in the exhaust gas, the emission index can be expressed as:

$$EI_{NOx} = \frac{\chi_{NOx}}{\chi_{CO} + \chi_{CO2}} \cdot \frac{n \cdot M_{NOx}}{M_f} \tag{3}$$

Here, n represents the number of carbon atoms in the fuel molecule, and M_i is the molar mass of the respective substance.

Fig. 14 illustrates the variations in CO and NOx emissions versus the adiabatic flame temperature for both the inline (0° config.) and the staggered/inclined (20° config.) arrangements. The adiabatic flame temperature was computed using a detailed chemical equilibrium model, considering defined pressure, air inlet temperature, fuel/air ratio, and kerosene inlet temperature, while also accounting for the enthalpy of vaporization. Plotting the Emission Index (EI) against T_{ad} facilitates comparisons of different operating points at similar combustion temperatures, assuming complete premixing. Discrepancies in EI at the same T_{ad} can be attributed to variations in the degree of premixing. It can be inferred that, for a given adiabatic flame temperature, differing NOx concentrations result from factors such as varying droplet evaporation rates, differences in premixing, or alterations in the lift-off zone length, rather than variations in the mean adiabatic flame temperatures.

Fig. 14(a) illustrates the impact of air inlet temperature on the NOx emissions in both inline and inclined configurations. In this figure, air inlet temperatures are represented by similar colors, with solid lines denoting the inline case and dashed lines for the inclined configuration. At low air inlet temperatures (290 K and 373 K) the fuel evaporation is rather slow with short LOH for that reason the advantages of lifted flames regarding NOx reduction are not fully exploited. Increasing the air inlet temperature (up to 473 K) rapidly lowers the overall NOx emissions due to longer LOH and fast evaporation and accordingly improvement of the homogeneity.

It is recognized that multiple mechanisms contribute to the formation of nitrogen oxides (NOx) in gas turbines. However, it is widely acknowledged that the Zeldovich mechanism serve as the primary source of NOx production, particularly at high temperatures. This theory finds substantial support in the observations that a substantial increase in adiabatic flame temperature results in a corresponding rise in NOx emissions across all the configurations and conditions examined.

Additionally, it becomes evident that the inclined configuration exhibits slightly better NOx emission performance, particularly under real operating conditions. This is attributed to its extended Lift-Off Height (LOH) and, conversely, a reduced extent of outer recirculation, which collectively contribute to the overall improvement in emissions.

The CO emissions are shown in Fig. 14(b) for the same operating points as the NOx emissions. If the adiabatic combustion temperature is reduced further after the steep increase of CO, the flame blows off. At low inlet temperatures, a more diffusion type flame behavior can be seen. The flame is partly quenched and the CO emissions are just rising steadily before flame extinction. With higher inlet temperatures and related higher degree of pre-evaporation and premixing low EI_{CO} emissions are achieved. At elevated combustion temperatures, CO emissions increase due to the dissociation of CO_2 into CO. This phenomenon is ascribed to the heightened thermal energy levels at elevated temperatures, which facilitate the generation of CO through the breakdown of CO_2. The dissociation reaction of CO_2 into CO and atomic oxygen (O) is endothermic, requiring the absorption of heat. Consequently, in environments with high adiabatic flame temperatures, the thermal energy available drives this dissociation process, resulting in an elevated CO concentration in the combustion products.

4. Conclusions

In conclusion, the objective of this investigation was to evaluate the operational performance of a gas turbine model combustor equipped with a lean liquid fuel injection system. The primary goal was to obtain a comprehensive understanding of flame behavior, stability factors, and emission performance under a variety of operating scenarios. Optical diagnostics, including PIV, Mie scattering, and OH* chemiluminescence, in combination with local probe measurements for temperature

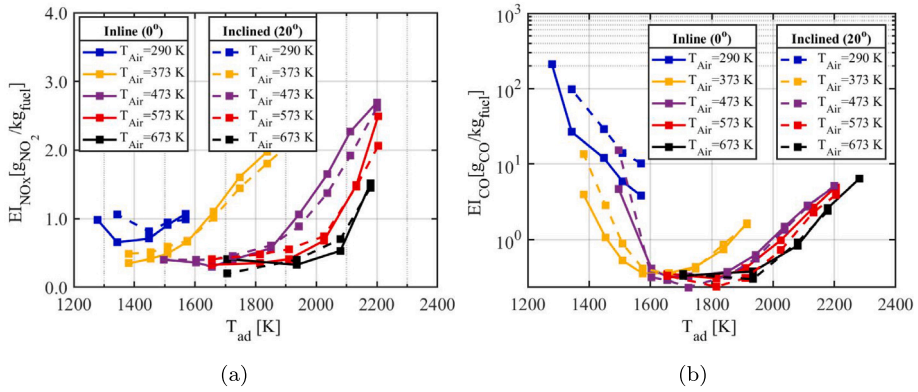

Fig. 14. Influence of adiabatic flame temperature on emissions at 3% air pressure drop for inline and inclined/staggered configurations.

and exhaust gas composition, were employed to replicate real-world aeronautic propulsion conditions marked by low swirl levels and high air inlet temperatures.

The results obtained revealed the remarkable stability of low swirl, lifted flames in comparison to conventional moderate swirl flames with larger inner recirculation zones. Additionally, the inline arrangement surprisingly demonstrated slightly higher stability than the inclined arrangement, each relying on distinct stabilization mechanisms. The flow field structure in the inline configuration was primarily governed by Outer Recirculation Zones (ORZ) at the sides of individual burners, with the size and location of these ORZs dependent on the ratio of air inlet temperature to adiabatic flame temperature. The recirculation zones facilitated flame anchoring, acted as radical pools and thermal reservoirs, and enhanced heat transfer, leading to increased flame speed and turbulence levels, contributing to improved flame stability. Conversely, in the inclined configuration, temperature profiles indicated an unexpected decrease in flow temperature near the wall, attributed to recirculated airflow from the upper to the lower burner. At low air inlet temperatures, resembling idle engine conditions, the flame stabilization mechanism relied on the slow evaporation of fuel droplets, resulting in the formation of local rich pockets near the flame root in both inline and inclined configurations.

By utilizing OH* chemiluminescence and Mie scattering techniques, we examined the size and location of heat release rates under various operational conditions. At lower air inlet temperatures, OH* chemiluminescence images revealed distinct high-luminosity heat release regions on each side of the nozzle center, attributed to the outward movement of droplets near the shear layer. This effect results from the lower T_{air} air and delays the evaporation of droplets. The results indicated that, at lower temperatures and across all configurations, the flame stabilizes at a closer distance above the nozzle exit due to the presence of local rich pockets near the shear layer. Furthermore, for a given tilt angle, the flame lift-off height increases with higher air inlet temperatures, leading to faster evaporation and enhanced mixing. This increased mixing aligns with the observed stability mechanism. Additionally, increasing the air inlet temperature to a specific point (dependent on each tilt angle) leads to a lower ratio of flow velocity to burning velocity, causing the flame to adapt and move downstream.

Exhaust gas analyses were conducted to assess the emission performance of the multi-burner arrangement. The results demonstrated that these lifted flames consistently produced very low NOx emissions across a wide range of operational conditions for all configurations studied.

In summary, the findings of this study carry significant implications for the future development and optimization of lean combustion technology for aircraft engines. The investigation highlighted the low NOx emissions associated with the lifted low swirl spray flames across a wide range of operational conditions, offering advantages compared to moderate swirl configurations. Furthermore, the drawbacks of an unwanted flow deflection for staggered/inclined burner arrangement, which is associated to swirled flows, are avoided. These discoveries are expected to facilitate the advancement and optimization of low swirl lean combustion technology for aircraft engines, offering advantages over moderate swirl configurations.

CRediT authorship contribution statement

Mohamed Shamma: Writing – review & editing, Writing – original draft, Visualization, Validation, Formal analysis, Data curation. **Stefan Harth:** Writing – review & editing, Visualization, Validation, Supervision, Project administration, Funding acquisition, Conceptualization. **Dimosthenis Trimis:** Writing – review & editing, Supervision, Project administration, Conceptualization.

Declaration of competing interest

The authors declare that they have no known competing financial interests or personal relationships that could have appeared to influence the work reported in this paper.

Data availability

Data will be made available on request.

Acknowledgments

This project has received funding from the Clean Sky 2 Joint Undertaking (JU) under grant agreement No. 831881 (CHAiRLIFT). The JU receives support from the European Union's Horizon 2020 research and innovation programme and the Clean Sky 2 JU members other than the Union. The authors would like also to thank the German Research Foundation (DFG) for the financial support of measuring instruments within the HBFG program (INST 121384/178-1 FUGG).

Appendix. Supplementary data

See Fig. A.15.

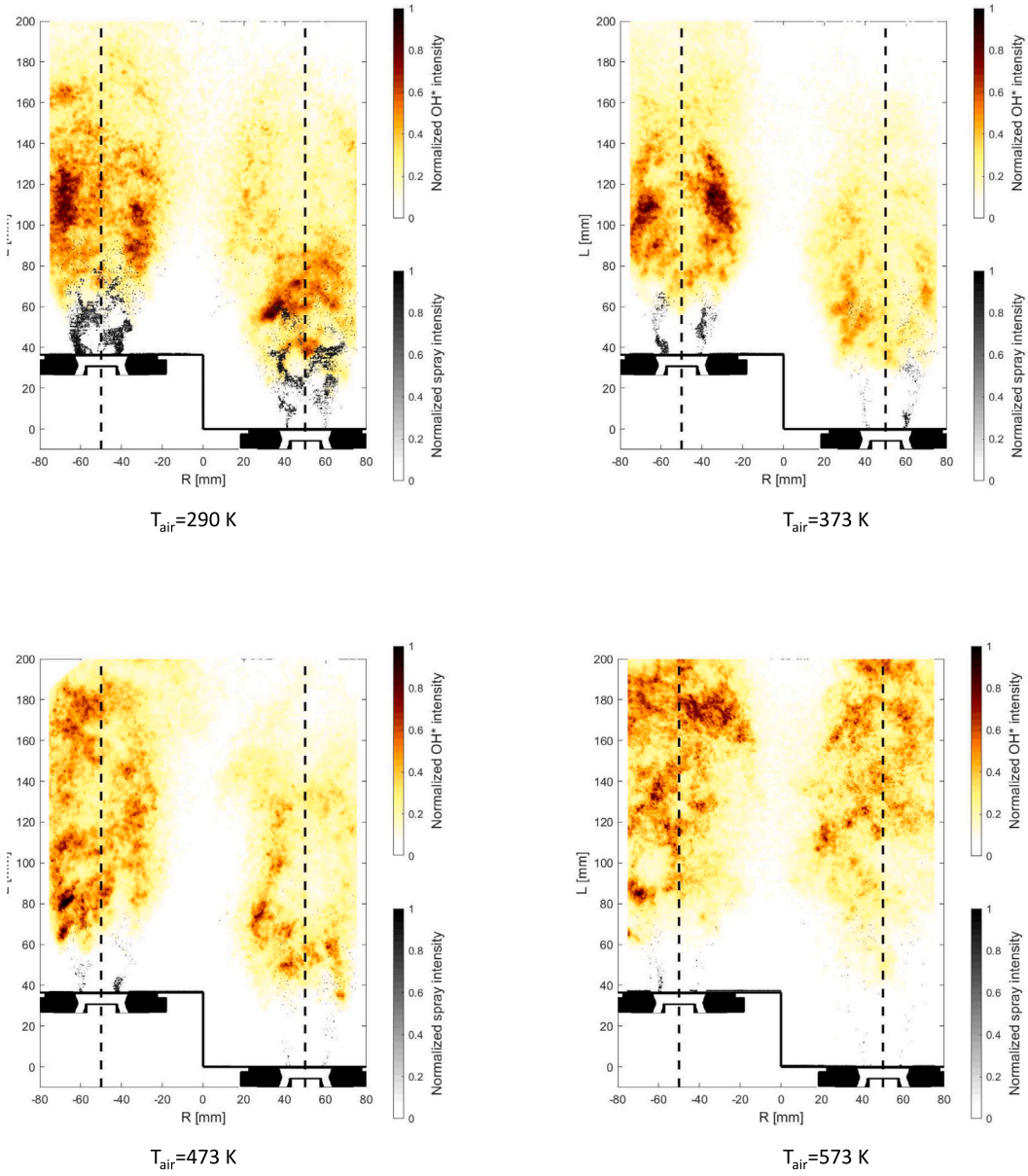

Fig. A.15. Visualization of the instantaneous OH* field overlaid onto instantaneous spray dispersion, obtained through Mie scattering measurements, for a staggered configuration with a constant equivalence ratio ϕ of 0.5 and a relative pressure drop $\frac{\Delta p}{P_2}$ of 3%, captured at various air inlet temperatures.

References

[1] Darecki M, Edelstenne C, Enders T, Fernandez E, Hartman P, Herteman J, et al. Flightpath 2050, flightpath 2050 eur. Vis Aviat 2011;28.

[2] Lefebvre AH. The role of fuel preparation in low-emission combustion. 1995.

[3] Correa SM. Power generation and aeropropulsion gas turbines: From combustion science to combustion technology. In: Symposium (international) on combustion, vol. 27, no. 2. Elsevier; 1998, p. 1793–807.

[4] Gupta AK, Lilley DG, Syred N. Swirl flows. Tunbridge Wells 1984.

[5] Chigier N, Beer J. Velocity and static-pressure distributions in swirling air jets issuing from annular and divergent nozzles. 1964.

[6] Tsao J, Lin C. Reynolds stress modelling of jet and swirl interaction inside a gas turbine combustor. Internat J Numer Methods Fluids 1999;29(4):451–64.

[7] Stone C, Menon S. Swirl control of combustion instabilities in a gas turbine combustor. Proc Combust Inst 2002;29(1):155–60.

[8] Anacleto P, Fernandes E, Heitor M, Shtork S. Swirl flow structure and flame characteristics in a model lean premixed combustor. Combust Sci Technol 2003;175(8):1369–88.

[9] Huang Y, Yang V. Effect of swirl on combustion dynamics in a lean-premixed swirl-stabilized combustor. Proc Combust Inst 2005;30(2):1775–82.

[10] Linck MB, Gupta AK. Twin-fluid atomization and novel lifted swirl-stabilized spray flames. J Propuls Power 2009;25(2):344–57.

[11] Syred N, Beer J. Combustion in swirling flows: a review. Combust Flame 1974;23(2):143–201.

[12] Johnson M, Littlejohn D, Nazeer W, Smith K, Cheng R. A comparison of the flowfields and emissions of high-swirl injectors and low-swirl injectors for lean premixed gas turbines. Proc Combust Inst 2005;30(2):2867–74.

[13] Cheng RK, et al. Low swirl combustion. Gas Turbine Handb 2006;241–55.

[14] Law C. Twenty-second symposium (international) on combustion. Pittsburgh: The Combustion Institute; 1988.

[15] Broadwell JE, Dahm WJ, Mungal MG. Blowout of turbulent diffusion flames. In: Symposium (international) on combustion, vol. 20, no. 1. Elsevier; 1985, p. 303–10.

[16] Peters N, Williams FA. Liftoff characteristics of turbulent jet diffusion flames. AIAA J 1983;21(3):423–9.

[17] Singh G, Jayanandan K, Kourmatzis A, Masri A. Spray atomization and links to flame stability over a range of weber numbers and pressure ratios. Energy Fuels 2021;35(19):16115–27.

[18] Cabra R, Dibble RW, Chen J-Y. Characterization of liquid fuel evaporation of a lifted methanol spray flame in a vitiated coflow burner. Tech. rep., 2002.

[19] Shamma M, Hoffmann S, Harth SR, Zarzalis N, Trimis D, Koch R, et al. Investigation of adjacent lifted flames interaction in an inline and inclined multi-burner arrangement. In: Turbo expo: Power for land, sea, and air, vol. 84959. 2021, V03BT04A020.

[20] Ariatabar B, Koch R, Bauer H-J, Negulescu D-A. Short helical combustor: Concept study of an innovative gas turbine combustor with angular air supply. J Eng Gas Turbines Power 2016;138(3).
[21] Kasabov P, Zarzalis N, Habisreuther P. Experimental study on lifted flames operated with liquid kerosene at elevated pressure and stabilized by outer recirculation. Flow Turbul Combust 2013;90(3):605–19.
[22] Wollgarten JC, Zarzalis N, Turrini F, Peschiulli A. Experimental investigations of ion current in liquid-fuelled gas turbine combustors. Int J Spray Combust Dyn 2017;9(3):172–85.
[23] Hertzberg J, Shepherd I, Talbot L. Vortex shedding behind rod stabilized flames. Combust Flame 1991;86(1–2):1–11.
[24] Marinov S, Kern M, Zarzalis N, Habisreuther P, Peschiulli A, Turrini F, et al. Similarity issues of kerosene and methane confined flames stabilized by swirl in regard to the weak extinction limit. Flow Turbul Combust 2012;89(1):73–95.
[25] Vanquickenborne L, Van Tiggelen A. The stabilization mechanism of lifted diffusion flames. Combust Flame 1966;10(1):59–69.
[26] ARP1533-SAE. Procedure for the calculation of gaseous emissions from aircraft turbine engines. 1996.